International Journal of Engineering and Management Sciences (IJEMS) Vol. 8. (2023). No. 3.

DOI: 10.21791/IJEMS.2023.023

Prediction of FLD using Abaqus and Gurson Model for Simple Flat Specimen

DOMOKOS TATIANE[1], BAKSA ATTILA[2], SZÁVAI SZABOLCS[3]

[1]University of Miskolc, Faculty of Mechanical Engineering and Informatics, Institute of Applied Mechanics, metwadas@uni-miskolc.hu

[2]University of Miskolc, Institute of Applied Mechanics, attila.baksa@uni-miskolc.hu

[3]University of Miskolc, Institute of Machine and Product Design, szavai.szabolcs@uni-miskolc.hu

Abstract. In the past century, in many industries, such as, metal forming industry, it has been important to predict ductile damage and fracture of metals under complex loadings. Regarding damage mechanics, one of the most classical models is the Gurson-Tvergaard-Needleman, which was originated from Gurson and later enhanced by Tvergaard and Needleman. The inprovement was achieved by introducing an equivalent void volume fraction f and two more parameters called q_1 and q_2 into the yield function of Gurson's model.

Keywords: Forming limit diagram (FLD), Gurson model, metal forming, Abaqus

Introduction

Recently, there is a crescively interest of the automotive, aerospace, aluminium and steel industries in numerical simulation of the fracture process of typical structural materials. Conformably, there is an expectation that developers of commercial codes, such as ABAQUS, LS-DYNA and PAM-CRASH to implement reliable fracture criteria into those codes [4].

A trustworthy prediction of ductile failure in metals is still a matter of research and tests. Among several models, GTN has been used widely. The bigger limitation of Gurson-Tvergaard-Needleman is the difficulty to identify accurate parameters for the model. Due to the impossibility to perform experiments for their evaluation, inverse procedures are done aiming to estimate the material parameters of the GTN porosity-based plastic damage model by means of RSM (response surface methodology) method. The results showed good agreement between experimental and predicted forming limit diagram when determined GTN parameters were utilized. Finite Element (FE) simulation was done by Abaqus software to predict FLDs [1].

Nomenclature [3]

E, γ	Young's modulus and Poisson's ratio, respectively
$\bar{\sigma}_m, \bar{\varepsilon}_m^p, \dot{\bar{\varepsilon}}_m^p$	Equivalent stress of the matrix material, plastic strain of matrix material, and plastic strain rate of matrix material, respectively

DOI: 10.21791/IJEMS.2023.023

$\bar{A}, \bar{B}, \bar{C}$	Voce model parameters
$\sigma_{eq}, \sigma_m, \sigma_h$	Macroscopic von Mises equivalent stress, mean stress, and hydrostatic pressure, respectively
f, f^*	Current void volume fraction and equivalent void volume fraction, respectively
D, D^*	Current shear damage and equivalent shear damage, respectively
$D^{ef}_{tension}, D^{ef}_{shear}$	Effective tension damage and effective shear damage, respectively
q_1, q_2	Adjustment parameters in origin GTN model
q_3, q_4	Constants in shear mechanism
S_N, S'_N	Standard deviation in tensile mechanism and in shear mechanism, respectively
θ_L	Lode angle
$f_C, f_F, f_N, \varepsilon_N$	Tensile damage parameters
$D_C, D_F, f'_N, \varepsilon'_N, q_5$	Shear damage parameters
k_1, k_2	Hardening factors
K, G	Bulk modulus and shear modulus, respectively
$\dot{\lambda}, \emptyset$	Plastic multiplier and yield function, respectively
$I, \dot{\varepsilon}^p$	Second order unit tensor and macroscopic plastic strain rate tensor, respectively
C, n	Fourth-order elastic tensor and plastic flow direction, respectively
$\boldsymbol{\sigma}$, S	Cauchy stress tensor and stress deviator tensor, respectively

1. Gurson Model

Gurson Tvergaard Needleman (GTN) model, (Gurson, 1977; Tvergaard, 1981; Tvergard and Needleman, 1984) developed an analytical model that predicts ductile fracture.

GTN is a very conventional model applied in engineering to predict failure in materials, such as, copper, aluminium and steel cast iron. GTN is an analytical model that predict fracture of the basis of nucleation, evolution and agglomeration of voids in materials [1]. The definition of the GTN model is:

$$\Phi(\sigma, f) = \left(\frac{\sigma_{eq}}{\bar{\sigma}_m}\right)^2 + 2q_1 f^* \cosh\left(\frac{3}{2}\frac{q_2\,\sigma_m}{\bar{\sigma}_m}\right) - 1 - (q_1 f^*)^2 = 0 \quad (1)$$

or

$$\Phi = \frac{\sigma_e^2}{\sigma_M^2} + 2q_1 f^* \cosh\left[\frac{\mathrm{tr}\sigma}{2\sigma_M}\right] - (1 + q_1^2 f^{*2})$$

Where, q_1 is the material constant, $tr\sigma$ is the sum of principal stresses, σ_M is the equivalent flow stress and f is the ratio of voids effective volume to the material ration

DOI: 10.21791/IJEMS.2023.023

$$f^*(f) = f_c \;\; If \; f \le f_c \tag{2}$$

$$f^*(f) = f_c + \frac{\left(\frac{1}{q_1}\right) - f_c}{f_f - f_c}(f - f_c) \;\; if \;\; f \ge f_c \tag{3}$$

Where, f is the voids' volume ratio, f_c is the voids' volume ratio at the beginning of nucleation, f_f is the voids' volume ration when fracture occurs and σ_M is the equivalent flow stress and it is obtained from the following work hardening relation:

$$\sigma_M\left(\varepsilon_M^{pl}\right) = \sigma_y\left(\frac{\varepsilon_M^{pl}}{\varepsilon_y} + 1\right)^n \tag{4}$$

Where, n is the strain-hardening exponent and ε_M^{pl} is the equivalent plastic strain.

The voids' growth rate is the sum of existing voids growth $\dot{f}_g$ and the new voids' nucleation $\dot{f}_n$

$$\dot{f} = \dot{f}_n + \dot{f}_g \tag{5}$$

The components formulated:

$$\dot{f}_g = (1 - f)tr\dot{\varepsilon}^{pl} \tag{6}$$

$$\dot{f}_n = A\dot{\varepsilon}_M^{pl} \tag{7}$$

$$A = \frac{f_n}{S_n\sqrt{2\pi}} exp\left[-\frac{1}{2}\frac{\varepsilon_M^{pl} - \varepsilon_N}{(S_N)}\right] \tag{8}$$

Where, $tr\dot{\varepsilon}^{pl}$ $(\varepsilon_x + \varepsilon_y + \varepsilon_z)$ is the volume plastic strain rate, S_N is the voids' nucleation mean quantity, fn is the volume ratio of the second phase particles (responsible for the voids' nucleation) and ε_N is the mean strain at the time of voids' nucleation.

GTN model involves eight parameters which can be defined in a vector from by

$$\Phi = \Phi(q_1, q_2, f_0, f_c, f_f, f_n, \varepsilon_N, S_N) \tag{9}$$

2. FLD – Forming Limit Diagram

A Forming Limit Diagram (FLD) is a graph which depicts the major strains ($\mathcal{E}_1$) for all values of the minor strain ($\mathcal{E}_2$) at the onset of localized necking. Normally, the determination of FLD means experiments requires much time and special equipment and for that reason, researchers have developed analytical and numerical models as an alternative for coping with the difficulties. As a matter of knowledge related to engineering, the GTN approach is one well known and used mesomechanical models for ductile fracture. However, the correct identification of the GTN model parameters is crucial for successful analysis of the ductile failure through GTN damage model. For the identification of those parameters, a suitable design of experiments strategy should be carried out [2].

3. Fracture toughness test

One example of determination of the GTN parameters is the use of the fracture toughness test, as it can be seen in the figure 1. This test can be performed on compact tension specimens [1].

DOI: 10.21791/IJEMS.2023.023

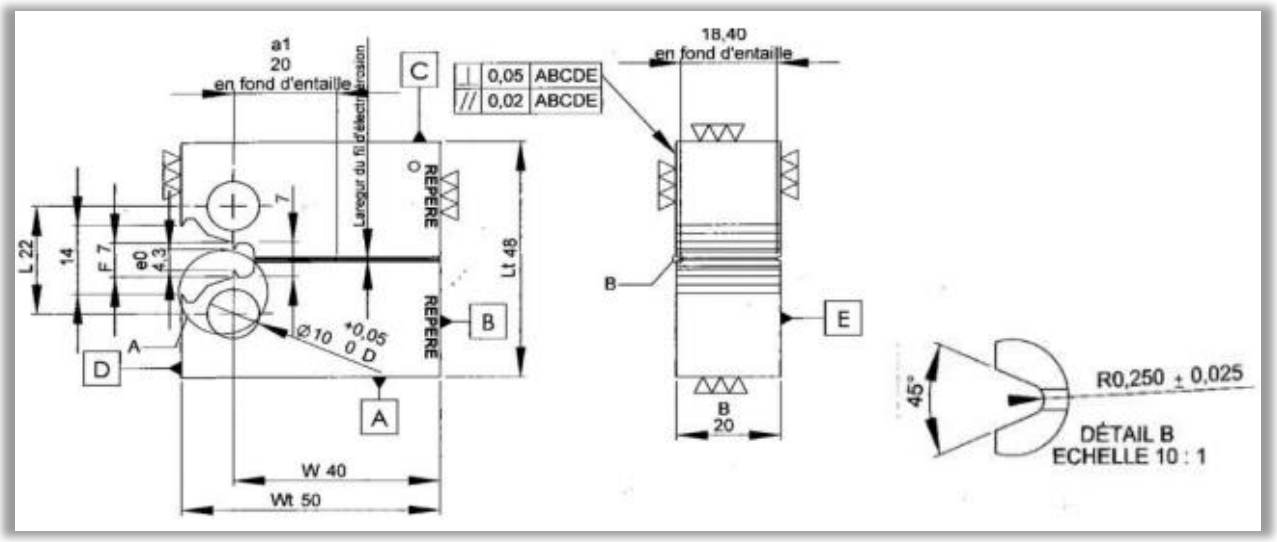

Figure 1. A CT specimen

According to the literature it is possible to have initial values of GTN parameters as showed in the table 1 below [1].

Table 1. Gurson parameters

References	q_1	q_2	E_N	S_N	f_0	f_F	f_N	f_C	Material	Comment
Bauvineau et al. (1996)	1.5	1	-	-	0.002	-	-	0.004	CMn steel	
Decamp et al. (1997)	1.5	1	-	-	0.0023	0.225	-	0.004	CMn steel	Uniaxial tensile test at 300°C on axisymmetric notched specimens
Siegmund et al. (1998)	1.5	1	0.3	0.1	0.0025	-	0.02	0.021	E460 steel	
Schmidt et al. (1997)	1.5	1	0.3	0.1	0	0.212	0.002	0.06	Ferritic steel base	Uniaxial tensile test at ambient temperature
	1.5	1	0.3	0.1	0	0.197	0.002	0.04	HAZ Ferritic	

DOI: 10.21791/IJEMS.2023.023

	1.5	1	0.3	0.1	0	0.189	0.012	0.03	Austenitic steel cladding CMn steel	
Skallerad and Zhang (1997)	1.25	1	0.3	0.1	0.0003	0.15	0.006	0.026	CMn steel	Tensile test
Benseddiq and Imad (2008)	1.5	1	0.3	0.1	~0	~0.2	0.002-0.02	0.004-0.06		

4. Sheet metal forming

Sheet metal forming is one of the most important manufacturing processes, which is affordable cost for mass production in industries. In order to have the conformation of sheet metal, it is necessary to convert thin and flat plates into parts of the desired shape and size, where the material will be subjected to large plastic deformations. Metal forming processes are classified into bulk forming processes and sheet metal forming processes. In both processes, the surface of the deforming metal and tools in contact and friction between them may have major effects on the material flow. The bulk forming processes are rolling, forging, wire drawing and extrusion. Sheet metal forming processes like deep drawing, stretching and bending are often used to produce a significant number of simple to complex components in automotive and aircraft industries, household appliances and others [7].

4.1. Basic concepts of Deep Drawing

Deep Drawing (DD) is the sheet metal forming process used to produce containers from flat circular blanks. The central portion of sheet of blank is subjected to pressure applied by punch into a die opening to get a sheet metal of desired shape without folding the corners. This normally requires the use of presses having a double action for blank holding force and punch force. Deep Drawing can also be explained as the combined tensile and compression deformation of a sheet to form a hollow body, without intentional change in sheet thickness [7].

4.2. Principle of Deep Drawing

A flat blank of sheet metal is formed into a cylindrical cup by forcing a punch against the centre portion of a blank that rests on the die ring. The blank can be circular, rectangular or a more abstract shape. Blank holder is loaded by a blank holder force, which is necessary to prevent wrinkling and to control the material flow into the die cavity simultaneously transferring the specific shape of the punch and the die to the blank. The material is drawn out of the blank holder-die region during the forming stage and the material is submitted to compressive and tensile stresses in this portion. The principle of deep drawing is represented in the Figure 2 [7].

DOI: 10.21791/IJEMS.2023.023

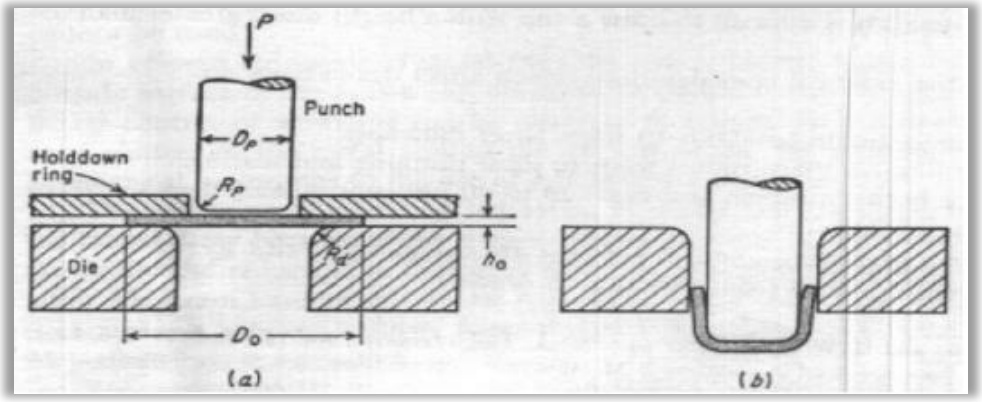

Figure 2. Deep drawing of a cylindrical cup (a) before drawing and (b) after drawing [7].

4.3. Common Defects in Deep Drawing

The three common defects that occur during DD are fracture, wrinkling and earing. Fracture occurs when the sheet metal is subjected to strains exceeding the safe strain limits of the material. For ductile sheets this fracture usually occurs near the punch corner. It is because maximum forming load appears in the material in this region and also stress concentration lines are converging in this section. Once this necking exceeds beyond a certain value, fracture appears in the drawn cup. A formed cup with a fracture at the cup bottom is shown in Figure 3 [7].

Figure 3. Fracture in deep drawing [7]

Wrinkling occurs in the flange when compressive stresses in the circumferential direction reaches a critical point of instability. It can occur in regions where the work piece is unsupported or when the blank holding force is insufficient. Wrinkling defect is shown in Figure 4. The wrinkling can be prevented by increasing blank holder force and by using a draw bead [5]. The draw bead bends and unbends the work piece material as it passes through the blank holder. This bending over the bead increases the radial tensile stresses and thus reduces the possibility of wrinkling [7].

DOI: 10.21791/IJEMS.2023.023

Figure 4. Wrinkling in deep drawing [7]

Deep drawing of anisotropic sheets results in a drawn cup with uneven top edge i.e. some kind of ears are formed at the top as shown in Figure 5. This defect is called earing and it is because of planar anisotropy of the blank material [7].

Figure 5. Earing in deep drawing [7]

Figure 6 shows the classification of deep drawing [7].

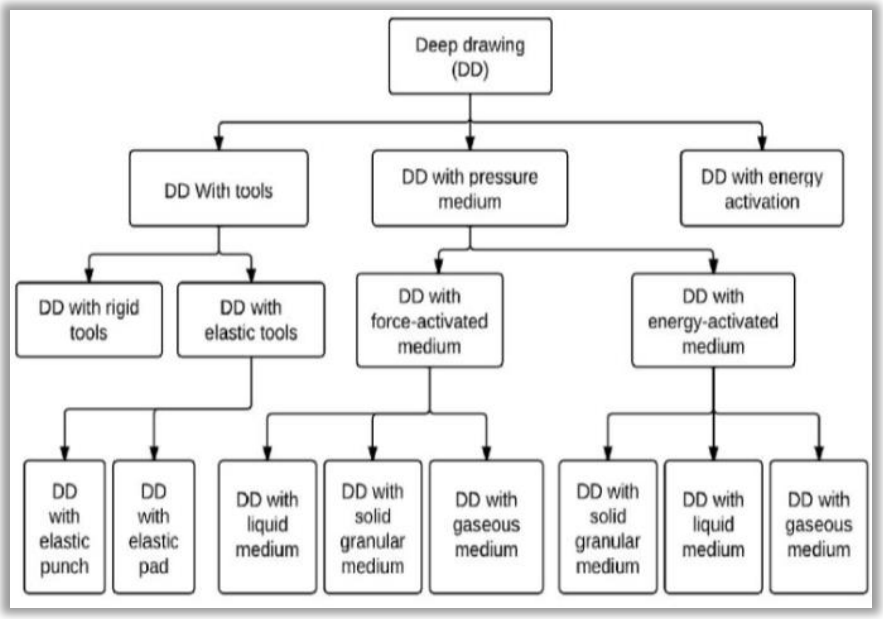

Figure 6. Classification of deep drawing

DOI: 10.21791/IJEMS.2023.023

5. Simulation on Abaqus

The Figure 7 represents a blank made of steel with 1 mm thickness and 100 mm length and Radius of 5 mm for punch, holder and die and figure 8 indicates the dimensions.

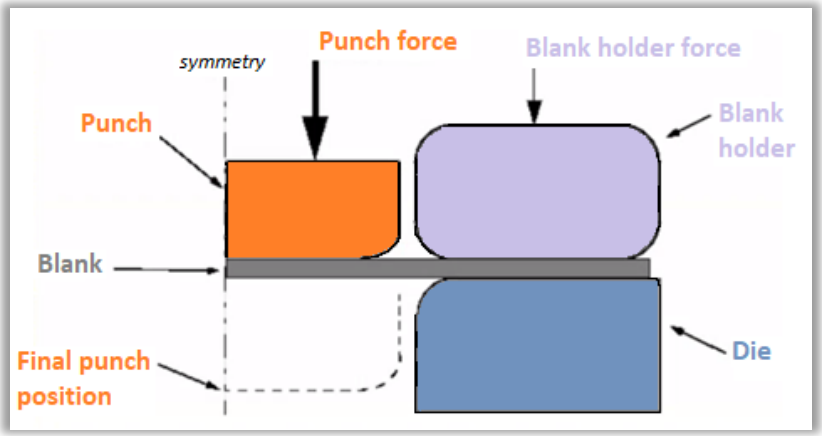

Figure 7. Blank of steel

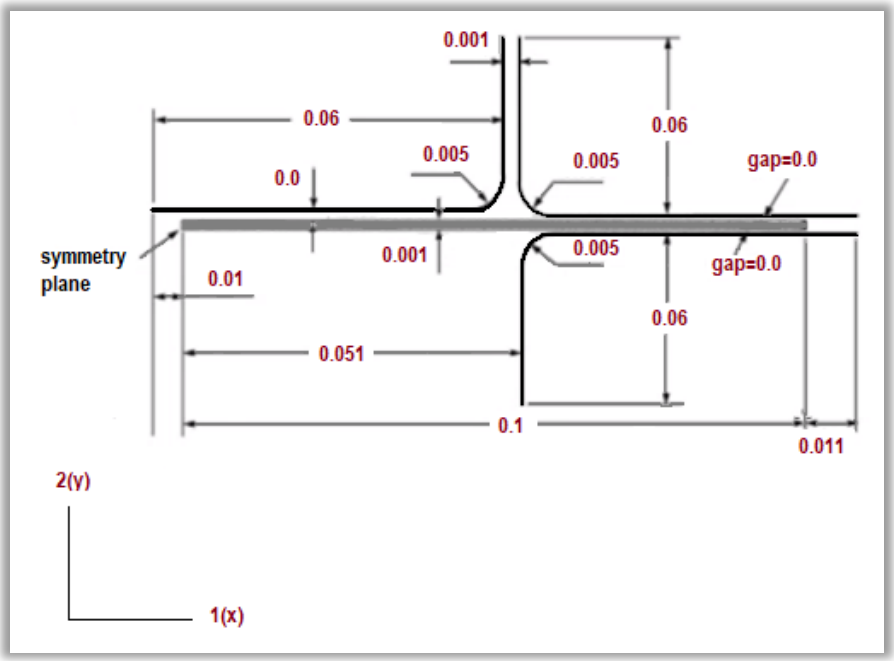

Figure 8. Dimensions for the blank, die, punch and holder

Table 3 indicates the values for the Yield stress and Plastic strain.

Table 3. Values for Yield stress and plastic strain

Yield stress (Pa)	Plastic strain (Ɛ)
400	0.0
420	0.02
500	0.2
600	0.5

DOI: 10.21791/IJEMS.2023.023

Figure 9 shows the Stress (MPa) x Plastic strain ($\mathcal{E}$). It can be seen the vertical line where is the ideal elastic and some linear hardening. The tensile strength is approximately 600 MPa.

The simulation on Abaqus is a good representation of the stress x strain relation.

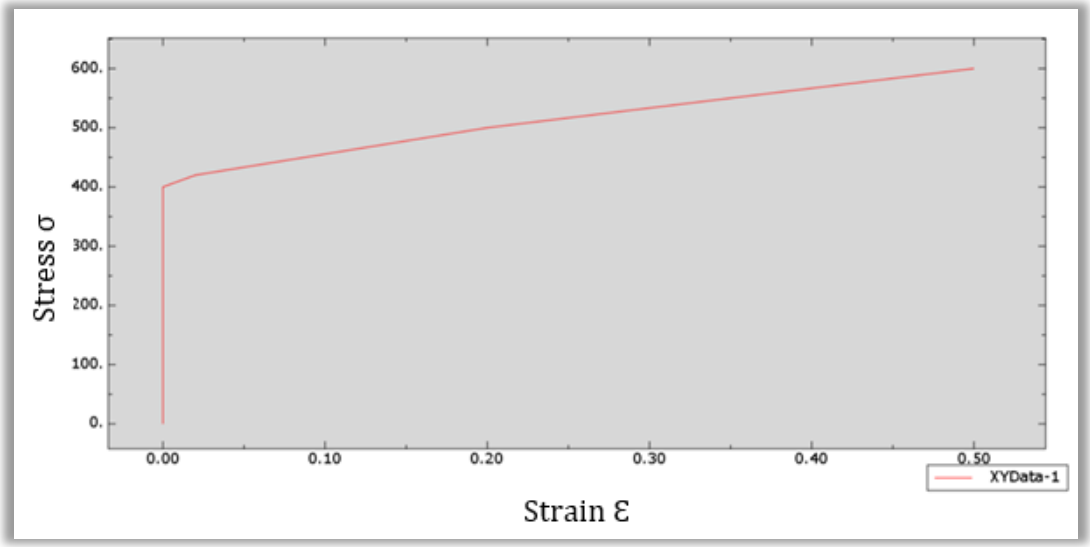

*Figure 9. Function Stress (*MPa*) x Plastic strain*

For this case the values of Young's modulus and Poisson's Ratio are 200000 and 0.3, respectively.

The Figure 10 shows the sketch for Punch, Blank, Holder and Die.

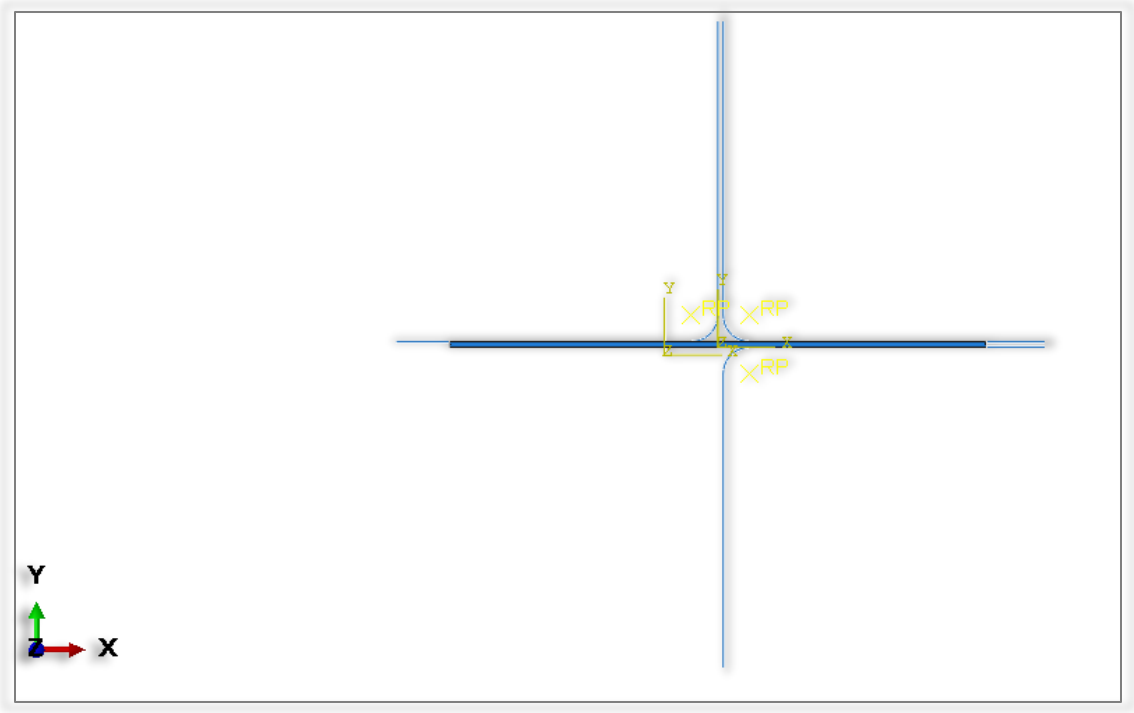

Figure 10. Sketch with the identification of the punch, blank, holder and die

Table 4 – values for holderforce

DOI: 10.21791/IJEMS.2023.023

Maximum number of increments		100		
		Initial	Minimum	Maximum
Increment size		0.05	1E-005	1

5.1. Results of the simulation

Figures 11 shows the result of the simulation where the deformation without rupture can be noticed.

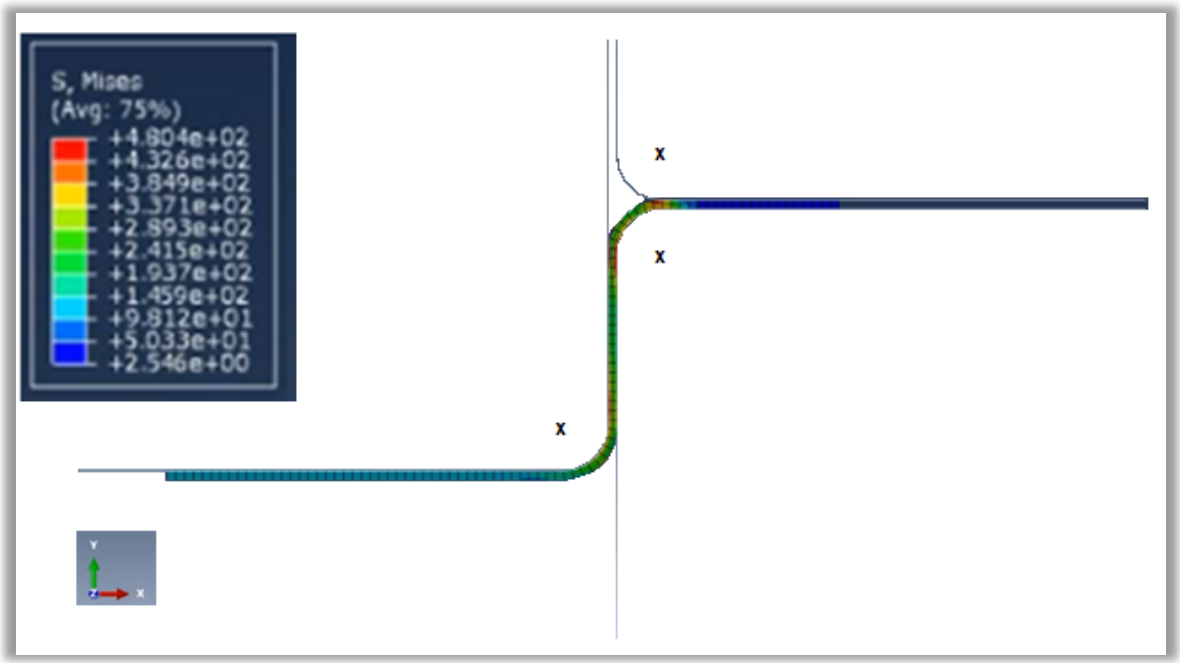

Figure 11. Final deformation

Figure 12 Shows the contact constraint stablization normal dissipation: ALLCCSDN for whole model

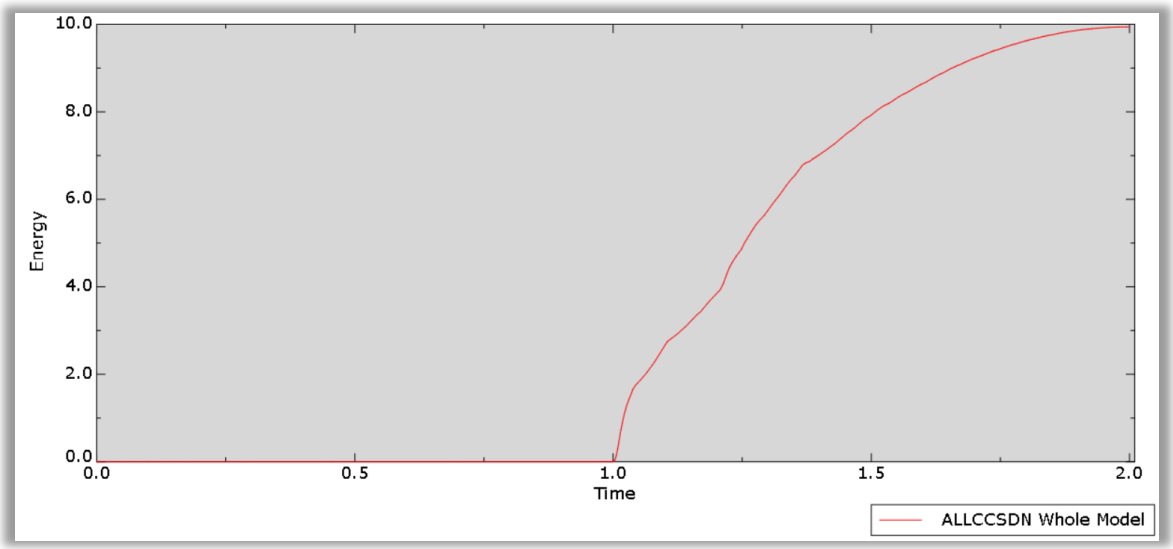

Figure 12. Contact constraint stabilization normal dissipation: ALLCCSDN for Whole Model

DOI: 10.21791/IJEMS.2023.023

Figure 13 shows the external work: ALLWK for Whole Model

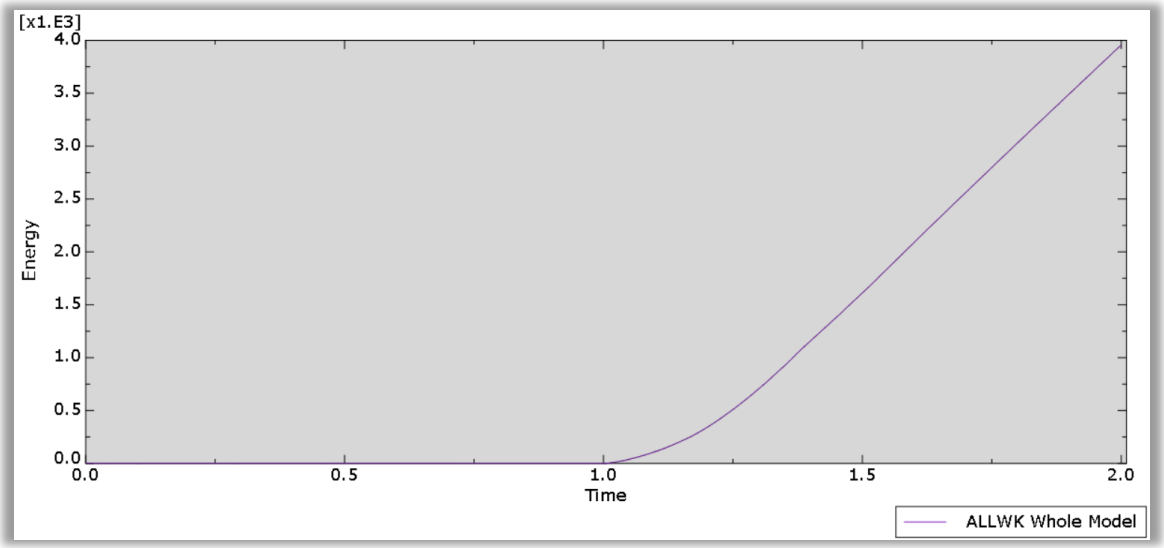

Figure 13. External work: ALLWK for Whole Model

Figure 14 shows the plastic dissipation: ALLPD for Whole Model

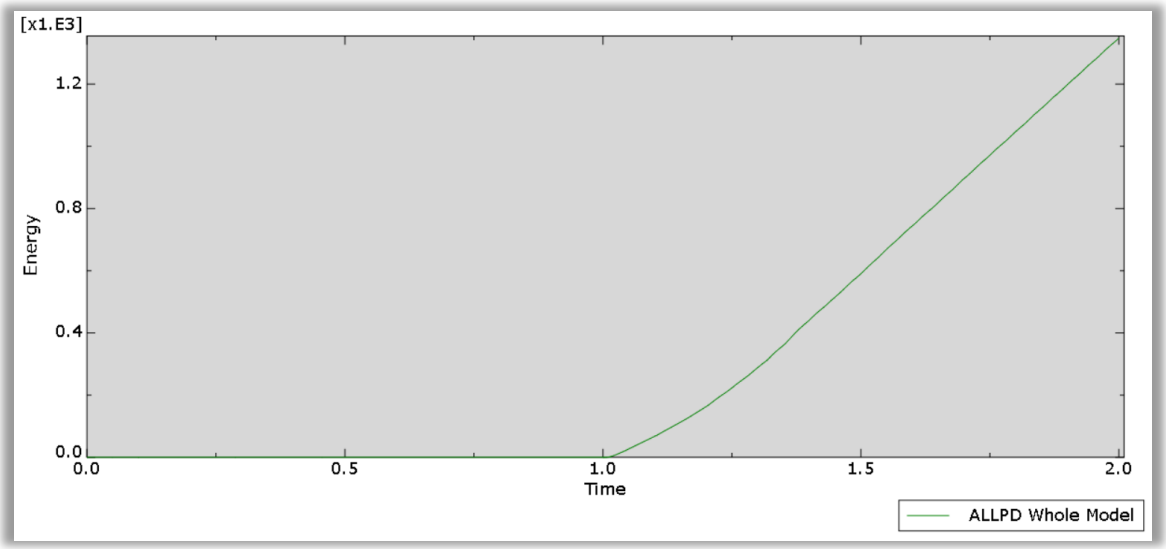

Figure 14. Plastic dissipation: ALLPD for Whole Model

DOI: 10.21791/IJEMS.2023.023

Figure 15 shows the Frictional dissipation: ALLFD for Whole Model

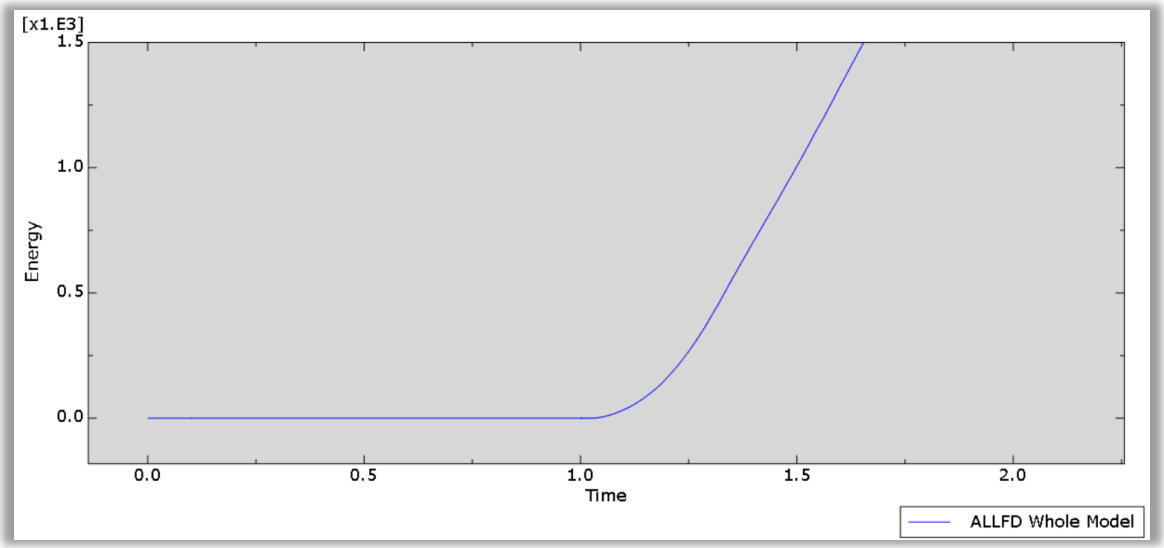

Figure 15. Frictional dissipation: ALLFD for Whole Model

5.2. Discussion and future plans

This paper shows an initial study where new simulations and experiments are planned to better understand the application of the Gurson method. In the future it is planned to do the test with DP600.

The process of crack creation in order to describe the behavior of the sheet metal during the punching process, interrupted tests at various levels of punch penetration should be performed. The specimens can be analyzed by SEM (Scanning Electron Microscopy) in order to better understand the mechanisms of deformation and fracture. Broberg showed that the damage is limited to a small region at the crack tip [5].

References

[1] Chahboub, Y., Szavai, S., Bezi, Z., *Determination of GTN Parameters of Sent Specimen During Ductile Fracture*, MultiScience – XXXIII. MicroCAD International Multidisciplinary Scientific Conference – University of Miskolc, Hungary, ISBN 978-963-358-177-3.

[2] Abbasi, M., Ketabchi, M., Izadkhah, H., Fatmehsaria, D.H., Aghbash, A.N., *Identification of GTN Model Parameters by Application of Response Surface Methodology. Science Direct. Procedia Engineering 10 (2011) 415-420.*

[3] Zao, H., Hao Z., Yumei, H., *An Improved Shear Modified GTN Model for Ductile Fracture of Aluminium Alloys Under Different Stress States and its Parameters Identification*, International Journal of Mechanical Sciences 192 (2021), 106081.

[4] Wierzbicki T, Bao Y, Lee YW, Bai Y. *Calibration and evaluation of seven fracture models*. International Journal of Mechanical Sciences 2005;47(4-5):719–43.

DOI: 10.21791/IJEMS.2023.023

[5] Achouri M, Germain G, Dal Santo P, Saidane D. *Experimental and numerical analysis of micromechanical damage in the punching process for High-Strength Low-Alloy steels*. Materials and Design 2014; 56:657–70.

[6] Rice JR, Tracey DM. On the ductile enlargement of voids in triaxial stress fields∗. Journal of the Mechanics Physics of Solids 1969;17(3):201–17.

[7] D.Swapna, Ch,Srinivasa Rao, S.Radhika. *A Review on Deep Drawing Process*. International Journal of Emerging Research in Management & Technology (June 2017), ISSN: 2278-9359 (Volume-6, Issue-6)

[8] Tvergaard V. *Influence of voids on shear band instabilities under plane strain conditions*. International Journal of fracture 1981;17(4):389–407.

[9] Benzerga AA, Leblond J-B. *Ductile fracture by void growth to coalescence*. Advances in applied mechanics 2010;44(10):169–305.

[10] Dowling NE. *Mechanical Behavior of Materials: Engineering Methods for Deformation*, Fracture, and Fatigue. Prentice Hall; 1993.

[11] Lemaitre J. A *Continuous Damage Mechanics Model for Ductile Fracture*. Transactions of the Asme Journal of Engineering Materials and Technology 1985;107(107):83–9.

[12] Sandoval C, Malcher L, Canut F, Araújo L, Doca T, Araújo J. *Micromechanical Gurson-based continuum damage under the context of fretting fatigue*: Influence of the plastic strain field. International Journal of Plasticity 2020; 125:235–64.